The Impact of Harness Impedance on Hall Thruster Discharge Oscillations

IEPC-2017-023

Presented at the 35th International Electric Propulsion Conference
Georgia Institute of Technology • Atlanta, Georgia • USA
October 8 -12, 2017

Luis R. Piñero[1]
NASA Glenn Research Center, Cleveland, Ohio, 44135, USA

Abstract: Hall thrusters exhibit characteristic discharge voltage and current oscillations during steady-state operation. The lower frequency breathing-mode current oscillations are inherent to each thruster and could impact thruster operation and PPU design. The design of the discharge output filter, in particular, the output capacitor is important because it supplies the high peak current oscillations that the thruster demands. However, space-rated, high-voltage capacitors are not readily available and can have significant mass and volume. So, it is important for a PPU designer to know what is the minimum amount of capacitance required to operate a thruster. Through SPICE modeling and electrical measurements on the Hall Effect Rocket with Magnetic Shielding (HERMeS) thruster, it was shown that the harness impedance between the power supply and the thruster is the main contributor towards generating voltage ripple at the thruster. Also, increasing the size of the discharge filter capacitor, as previously implemented during thruster tests, does not reduce the voltage oscillations. The electrical characteristics of the electrical harness between the discharge supply and the thruster is crucial to system performance and could have a negative impact on performance, life and operation.

Nomenclature

AC	=	alternating current
AEPS	=	Advanced Electric Propulsion System
BOB	=	break out box
C	=	capacitance
C_{DIS}	=	discharge filter capacitor
C_{DPS}	=	discharge power supply capacitor
C_H	=	harness capacitance
DC	=	direct current
f	=	frequency
HERMeS	=	Hall Effect Rocket Magnetic Shielding
I_{CDIS}	=	discharge filter capacitor current
I_{DIS}	=	discharge current
I_{DPS}	=	discharge power supply current
L	=	inductance
L_{DIS}	=	discharge filter inductor
L_H	=	harness inductance
P-P	=	peak-to-peak
PPU	=	power processing unit
PSD	=	power spectral density
R_H	=	harness resistance
RMS	=	root mean square
SEP	=	solar electric propulsion
V_{AND}	=	anode voltage
V_{CDIS}	=	discharge filter capacitor voltage
V_{HV}	=	vacuum harness voltage
V_{HA}	=	ambient harness voltage
VF	=	vacuum facility
X_{CH}	=	harness capacitive reactance
X_{LH}	=	harness inductive reactance
Z	=	impedance
Z_H	=	harness impedance

[1] Senior Electrical Engineer, Electric Propulsion Systems Branch, luis.r.pinero@nasa.gov

I. Introduction

Solar electric propulsion (SEP) is an enabling technology for near term and future NASA science and human exploration missions.[1-3] In 2012, Glenn Research Center and the Jet Propulsion Laboratory started development of a 14 kW Hall thruster and PPU that can serve as a building block for a 40 kW-class SEP system.[4] The in-house development resulted in the development of the 12.5 kW Hall Electric Rocket Magnetic Shielding (HERMeS) thruster that has demonstrated performance of more than 600 mN of thrust and specific impulse as high as 3,000 seconds.[5-8] The vacuum-compatible, HP-120/800V brassboard power processing unit (PPU) was also developed and demonstrated a peak efficiency in excess of 95 percent.[9-10] Both thruster and PPU were successfully integrated and used as a pathfinder for potential problems for advanced developments.

This effort has been transitioned to Aerojet Rocketdyne under the Advanced Electric Propulsion System (AEPS) contract which includes the development, qualification, and fabrication of multiple electric propulsion flight system strings which include thruster, PPU with integral digital control and interface functionality, xenon flow controller and harnesses.[11] While developing thruster and PPU requirements for the AEPS system, the question of how to specify discharge ripple emerged. Since both discharge voltage and current oscillations are intrinsic to the thruster design and can be affected by many variables, an effort was initiated to try to predict it through analysis or modeling. This paper summarizes the activities and findings of this effort.

II. Discharge Oscillations

Hall thrusters exhibit characteristic discharge voltage and current oscillations during steady-state operation. The frequency of these oscillations range from kHz to MHz and are caused by many processes including propellant ionization, magnetic field gradients, and plasma instabilities.[12] Significant attention must be paid to the lower frequency current oscillations, commonly known as breathing-mode oscillations, because they are typically the largest component. The low frequency of these oscillations can significantly impact the design of the discharge supply and its output filter, induce instabilities into the feedback loops and increase discharge voltage oscillations.

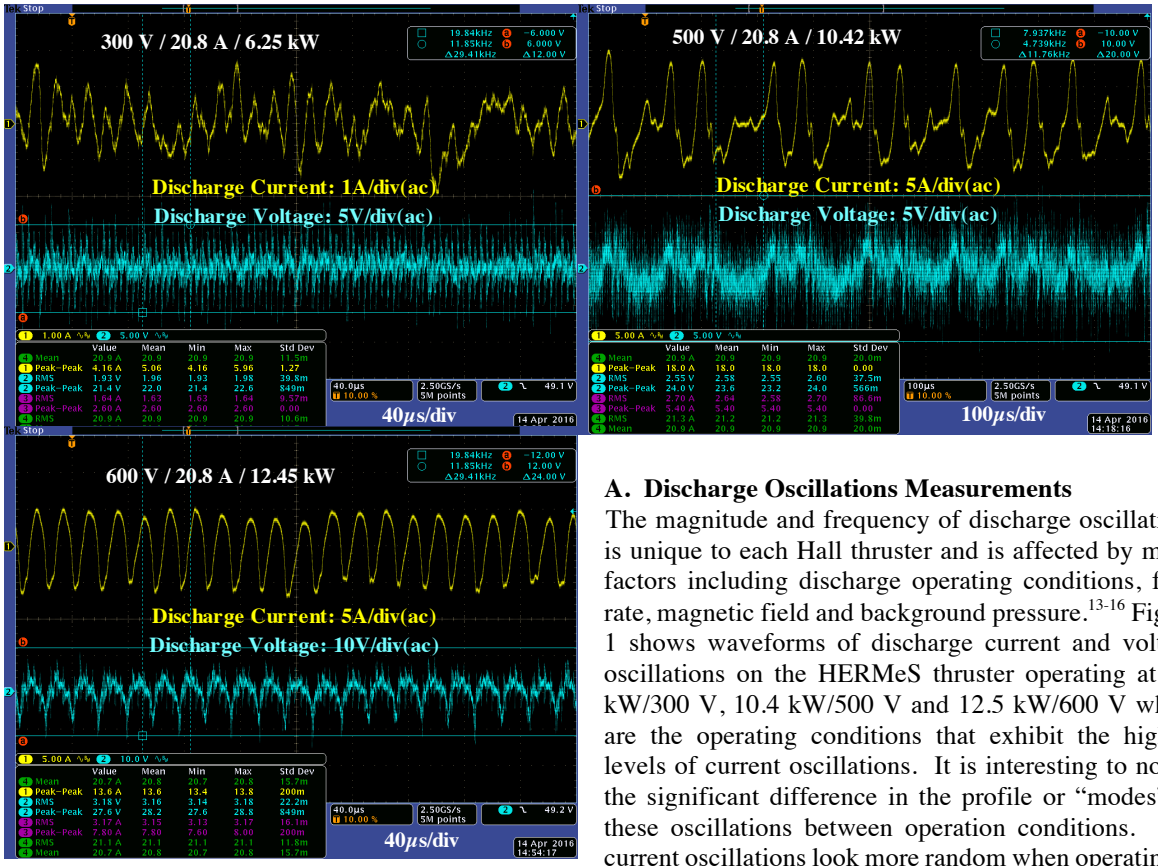

Figure 1. Waveforms discharge voltage and current oscillations

A. Discharge Oscillations Measurements

The magnitude and frequency of discharge oscillations is unique to each Hall thruster and is affected by many factors including discharge operating conditions, flow rate, magnetic field and background pressure.[13-16] Figure 1 shows waveforms of discharge current and voltage oscillations on the HERMeS thruster operating at 6.3 kW/300 V, 10.4 kW/500 V and 12.5 kW/600 V which are the operating conditions that exhibit the highest levels of current oscillations. It is interesting to notice the significant difference in the profile or "modes" of these oscillations between operation conditions. The current oscillations look more random when operating at 300 V but as the voltage increases they become more sinusoidal. Figure 2, shows the power spectral density

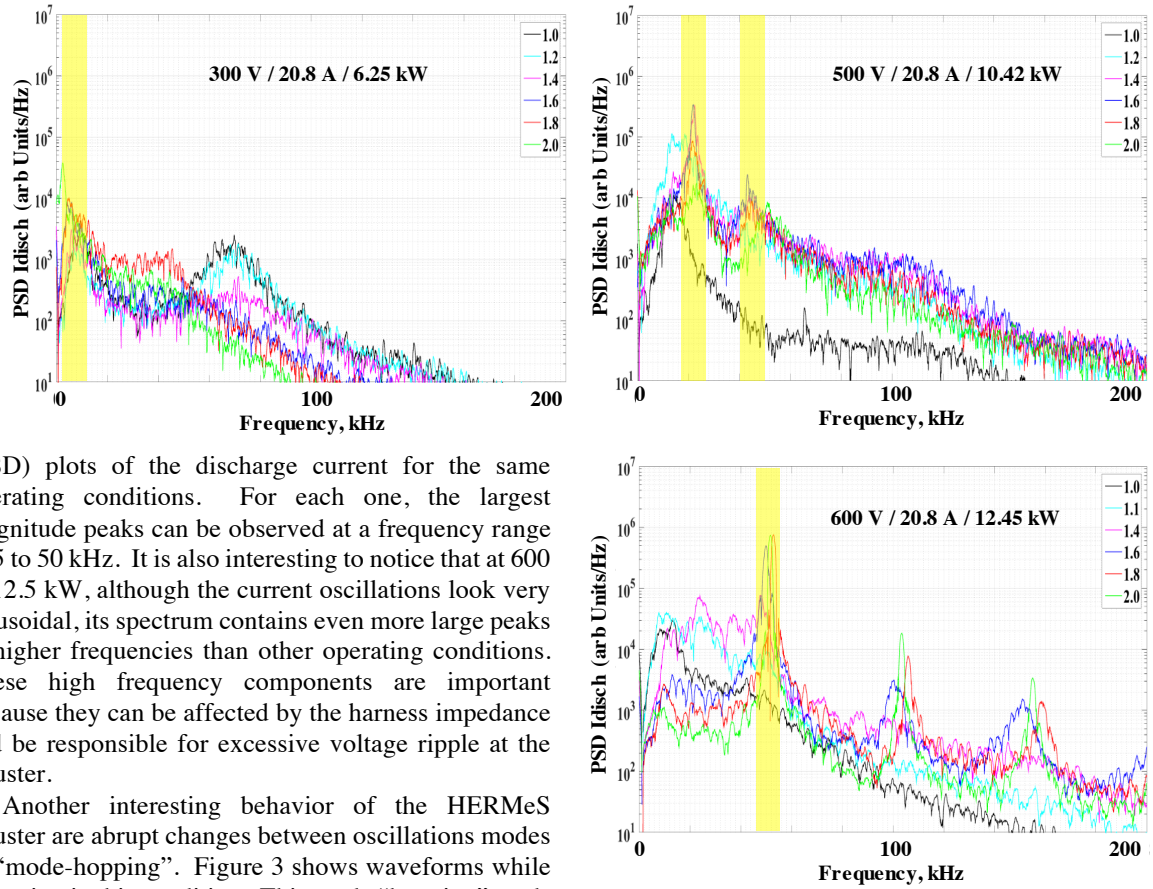

Figure 2. Power spectral density plots of discharge current oscillations

(PSD) plots of the discharge current for the same operating conditions. For each one, the largest magnitude peaks can be observed at a frequency range of 5 to 50 kHz. It is also interesting to notice that at 600 V/12.5 kW, although the current oscillations look very sinusoidal, its spectrum contains even more large peaks at higher frequencies than other operating conditions. These high frequency components are important because they can be affected by the harness impedance and be responsible for excessive voltage ripple at the thruster.

Another interesting behavior of the HERMeS thruster are abrupt changes between oscillations modes or "mode-hopping". Figure 3 shows waveforms while operating in this condition. This mode "hopping" tends to be more pronounced at higher magnetic field settings and its root cause is unknown. However, this behavior should also be taken in consideration in the PPU design.

B. Experimental Test Setup

Figure 4, shows a diagram of this basic test configuration used at GRC for Hall thruster testing. A commercial laboratory power supply or PPU provides discharge power to a thruster inside a vacuum chamber through a break-out-box (BOB) at the vacuum chamber wall. This BOB contains instrumentation to measure electrical power into the thruster and also provides a convenient location to add discharge filter capacitors (C_{DIS}) to mitigate discharge voltage ripple. This is particularly important when testing in the larger chambers like Vacuum Facility 5 (VF5) which has a diameter of 4.5 m or Vacuum Facility 6 (VF6) with a diameter of 7.5 meters. Very long electrical harnesses are typically required to deliver power to the thruster and these can impact discharge oscillations.

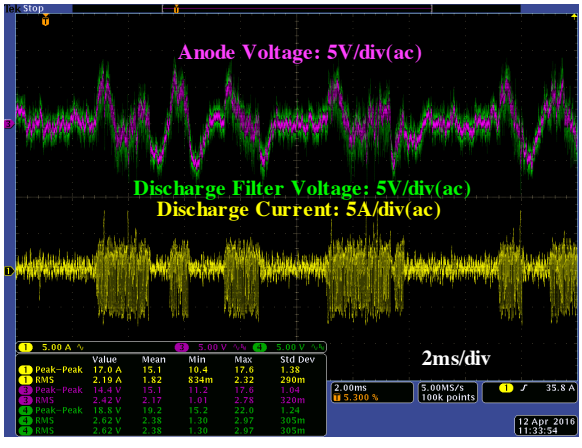

Figure 3. Thruster oscillations while "mode-hopping"

Every harness has an electrical impedance (Z) intrinsic to its design and construction. This impedance is determined by design parameters like conductor size, insulation, loop area between conductors and even placement with respect to ground. Electrical impedance is defined as:

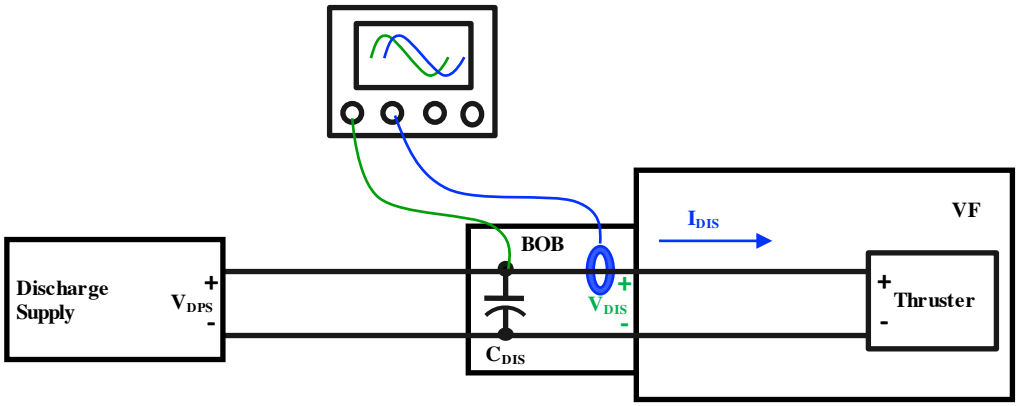

Figure 4. Basic test configuration at GRC

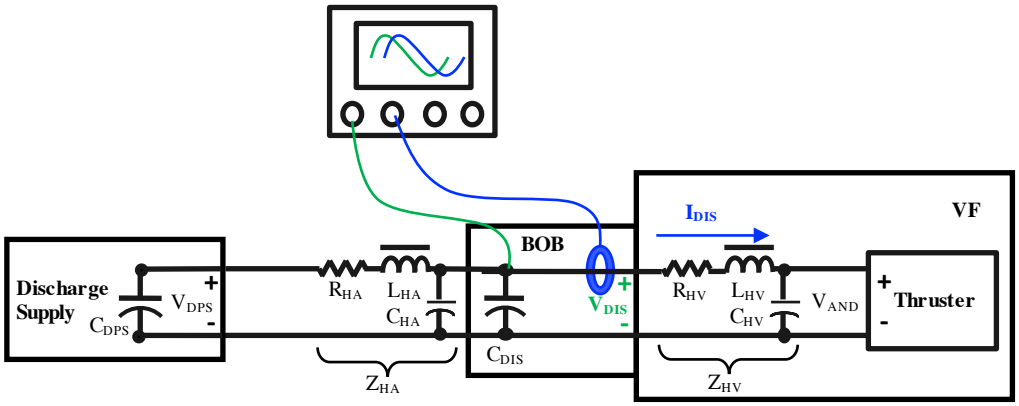

Figure 5. Test configuration with harness impedance components

$$Z = \sqrt{(R^2 + (X_L - X_C)^2)}$$

where:

$$X_L = 2\pi f L \quad \text{and} \quad X_C = 1/(2\pi f C)$$

which are the inductive and capacitive reactances that are a function of the inductance (L) and capacitance (C) and the frequency (f). Figure 5 shows the GRC basic test setup including the harness inductance (Z_H) as its three components including harness resistance (R_H), harness inductance (L_H) and harness capacitance (C_H) for both the vacuum and ambient portion of the harness. For a typical harness for this power level using twisted conductors as used at GRC, the "rule-of-thumb" values for these components are approximately 5 mΩ/m, 380 nH/m and 59 pF/m. R_H is typically small because harnesses are designed to minimize DC voltage drop so its contribution towards Z_H is very low. C_H is also typically very low because of the small surface area between conductors and the separation caused by the insulators equates to small capacitance. In addition, its contribution towards Z_H is inversely proportional to the frequency making it negligible at high frequency. Conversely, even when the harness conductors are twisted, L_H can be substantial and has significant impact towards Z_H because X_L is directly proportional to frequency. Since long harnesses are required inside VF5 and VF6, the harness inductance inside the vacuum chamber (L_{HV}) can have significant impact on thruster oscillations. There are no big concerns about the Z_{HA} of the harness on the atmospheric side of the vacuum chamber interface because its impedance components (R_{HA}, L_{HA} and C_{HA}) are very small compared to the added discharge filter components between the laboratory power supplies and the BOB.

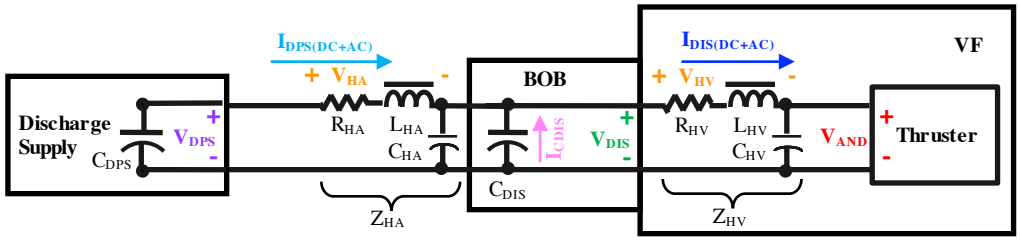

Figure 6. Discharge circuit analysis

C. Discharge Circuit Analysis

The discharge circuit of the Hall thruster experimental test setup is shown in Figure 6. The discharge current into the thruster has both DC and AC components. The DC component ($I_{DIS(DC)}$) is primarily supplied by the discharge supply ($I_{DPS(DC)}$) and only generates a small voltage drop along the harnesses because of their low R_H values. However, the AC component ($I_{DIS(AC)}$) is supplied by current (I_{CDIS}) from the discharge filter capacitor (C_{DIS}) in the BOB and also by current ($I_{DPS(AC)}$) from the output capacitors in the discharge supply (C_{DPS}). When a commercial laboratory power supply is used for discharge supply, $I_{DPS(AC)}$ can be significant even with the impact of the ambient harness impedance (Z_{HA}) because they typically have massive output filters to provide low output ripple and output impedance. Capacitors have a low X_C at high frequency which allows them to easily supply high frequency currents while generating a negligible voltage drop. For this reason, C_{DIS} helps reduce ripple at the BOB and eliminates the impact of the ambient harness on the discharge voltage at the thruster. However, once the voltage drop in C_{DIS} is negligible, indiscriminately increasing the size of this capacitor does not improve the voltage ripple at the thruster. On the vacuum-side of the circuit, $I_{DIS(AC)}$ generates a voltage drop along the vacuum harness impedance (V_{HV}) that makes the discharge voltage at thruster anode (V_{AND}) lower than the discharge voltage (V_{CDIS}) at C_{DIS} and induces voltage ripple at the anode. This is depicted in Figure 7 that shows the AC component of the V_{AND} (green) is significantly lower than V_{DIS} at the BOB (magenta).

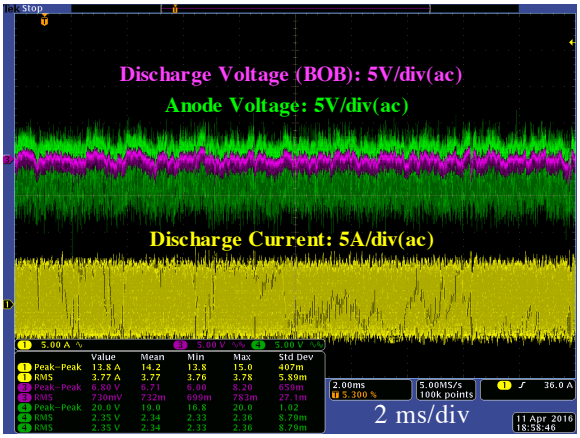

Figure 7. Voltage oscillations at thruster anode and BOB

D. Discharge Filter Capacitor Optimization

A test was conducted to find the minimum value of C_{DIS} needed at the BOB to maintain stable operation and low discharge voltage ripple on the HERMeS thruster. Figure 8 shows the complete configuration for this filter optimization test. A coaxial sense cable was added to accurately measure V_{AND} close to the thruster and the V_{CDIS} was measured at the BOB. Also, an isolated current probe was used to measure the I_{DIS} into the thruster. The C_{DPS} in the

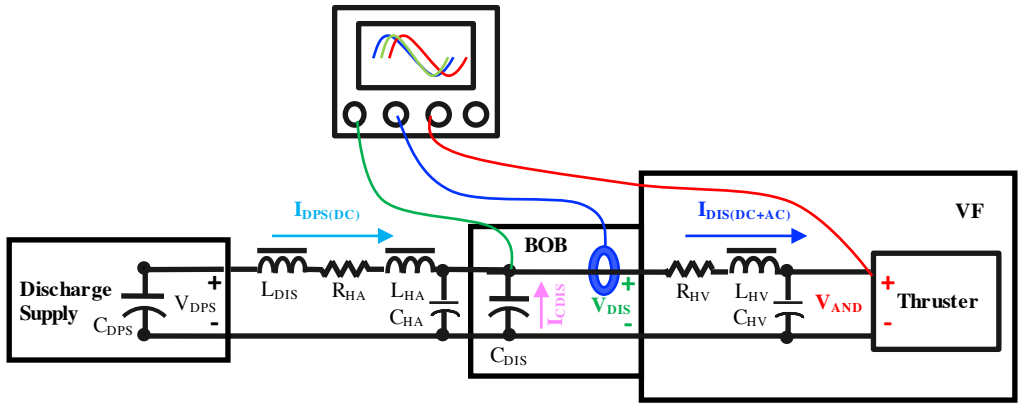

Figure 8. Test configuration for the filter optimization test

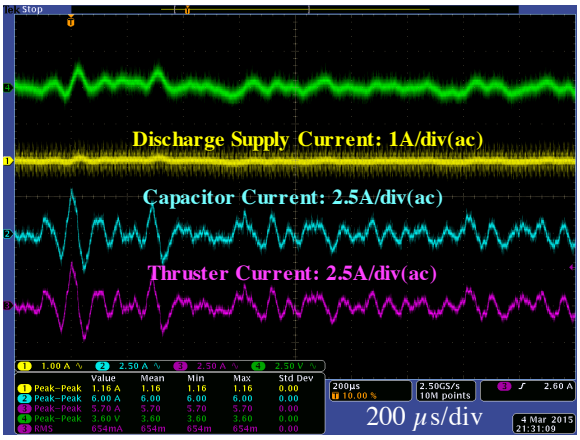

Figure 9. Thruster oscillations during filter optimization test

laboratory discharge power supply used for this test contained a large output filter capacitor, in the order of hundreds of mF, which is much larger than C_{DIS}. For this reason, C_{DPS} will contribute a significant part of $I_{DIS(AC)}$. To mitigate this effect, a large discharge filter inductor (L_{DIS}) was added between the output of the laboratory power supply and the BOB. The high X_L of this inductor forces $I_{DIS(AC)}$ to be primarily supplied by C_{DIS} and makes the test setup more representative of a typical PPU because they usually contain a limited amount of output filter capacitance for mass and volume reasons. Figure 9 shows voltage and current oscillation waveforms taken with this configuration. I_{CDIS} (blue) and $I_{DIS(AC)}$ (magenta) are basically identical while I_{DPS} (yellow) has very low ripple as expected. During the discharge filter capacitor optimization test, C_{DIS} was progressively reduced from 100 to 20 μF. Measurements of P-P and RMS voltages and currents were recorded. It was concluded that 30 μF was the minimum value of capacitance needed to satisfy the voltage ripple requirements. Below this value of capacitance, voltage ripple started to increase and for larger values it did not show a significant improvement. This reduction in discharge filter capacitance is important for PPU development because there is a limited selection of space-rated, high-voltage capacitors and their mass and volume can be significant.

III. Discharge Circuit Modeling

Previous efforts to model discharge oscillations have used a sinusoidal current source at the breathing-mode frequency to simulate the discharge current oscillations.[17] However, this is not appropriate for simulations to assess the effect of harness impedance because it does not contain the high frequency components that can add a significant contribution to the voltage oscillations. The new SPICE model created for this effort is shown in Figure 10. The discharge supply was modeled as a DC voltage source with a 300 mF output capacitance as in the laboratory discharge supply. Also included is a discharge filter with a 3 mH L_{DIS} and 30μF C_{DIS} as used in the BOB. A lumped element model was used to simulate the electrical harness in vacuum. This approach takes the distributed electrical attributes of the harness and concentrates them into single electrical components for resistance, inductance and capacitance. This simple model is valid for this case because the length of the harness is shorter than the wavelength of the discharge oscillations under consideration. The value for the harness components were measured in-place with an RLC meter. For the 6 m harness used in VF5, the R_{HV} was 32 mΩ, the L_{HV} was 2.5 μH and the C_{HV} was 236 pF. The thruster was modeled as a resistance that represents the I_{DC} and a programmable current source to represent the I_{AC}. This current source was programmed to match actual discharge current oscillations previously measured on a thruster using a high-bandwidth digital oscilloscope.

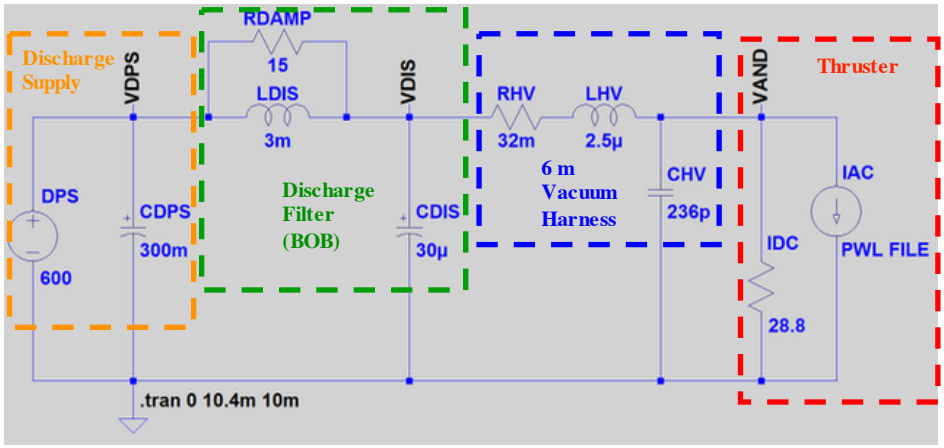

Figure 10. Lumped electrical harness model

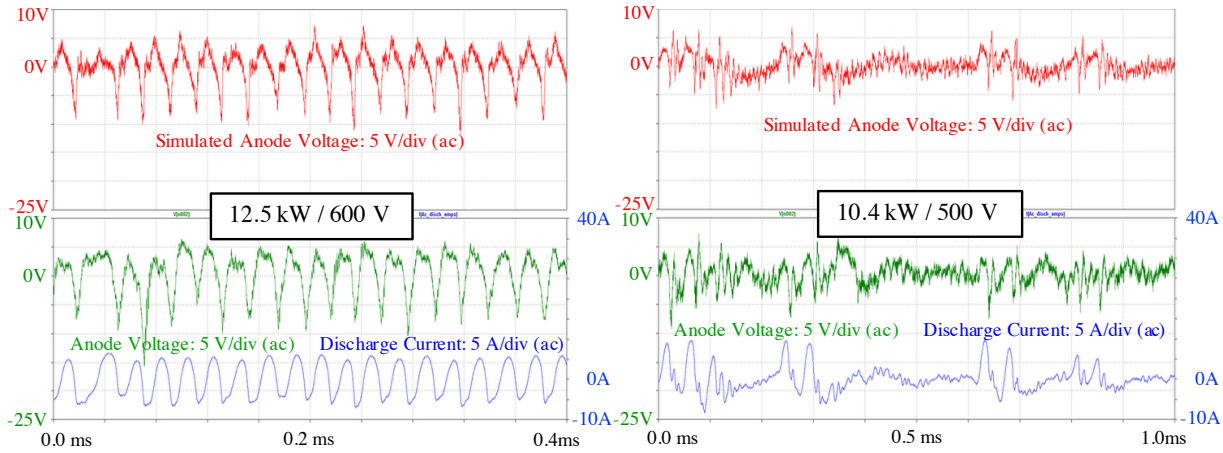

Figure 11. Simulated discharge voltage at thruster anode

The results of a transient analysis in SPICE are shown in Figure 11 for the 12.5 kW/600 V and 10.4 kW/500 V operating conditions. In both cases, the actual discharge voltage (green) look very similar to the simulated discharge voltage (red). The RMS and P-P values of the simulated discharge voltage ripple are within 14% of the actual values measured with the oscilloscope. The most significant finding from this result is that the discharge voltage ripple measured at the thruster is basically due to the voltage drop generated by the discharge current oscillations flowing through the harness impedance. The plasma itself does not seem to have much contribution toward the voltage ripple and behaves as a capacitive load. This result substantiates the importance of minimizing the harness inductance between a thruster and the discharge supply and filter in order to have low voltage ripple at the thruster anode.

IV. Low Inductance Harness

A. Low-Inductance Harness Options

There are several techniques that can be used to reduce the inductance between the thruster and the discharge supply. Table 1 summarizes some of the most common techniques including advantages and disadvantages of each. The discharge circuit model was used to assess the impact of reducing harness length and relocating the discharge filter capacitor location as potential options for the AEPS system. Calculations were done for operation at 12.5 kW / 600 V which had the highest level of voltage ripple. Figure 12 shows a plot of the P-P and RMS voltage ripple at the thruster as a function of harness length assuming a standard twisted-pair construction. The model predicts that at the maximum required length of 8 m, the P-P voltage ripple will be 21.3 V or 3.6% and the RMS voltage ripple 3.9 V or 0.7 percent. These values meet the most recent system specifications. Figure 13 shows a plot of the RMS and P-P voltage ripple at the thruster as a function of the location of the filter capacitor. Moving the capacitor closer to the thruster reduces the effective length of the harness and has the same effect as reducing its length. The P-P and RMS voltage ripples continuously improve down to a distance of 1 meter.

GRC implemented parallel-plate busbars in its large vacuum facilities (VF5 and VF6) to minimize discharge harness inductance. The busbars were built using two parallel 5 cm copper strips insulated with polyamide film and

Table 1. Inductance reduction techniques

Option	Pros	Cons
1. Minimize length	Low complexity	Limited by test setup
2. Twisted / braided wires	Low complexity	Limited effectiveness Impacts harness design (flexibility and cost)
3. Capacitor distance to thruster	Effective Insensitive to length Flight heritage	Mechanical, thermal and vacuum impacts on capacitor Can impact discharge output filter design
4. Coaxial cable	Low inductance	Difficult to implement for high power Limited flexibility
5. Parallel-plate busbar	Low inductance Easy to fabricate Scalable	Rigid Difficult to implement in spacecraft

fiberglass. This design resulted in an inductance of less than 20 nH/m and resistance of less than 2 mΩ/m. The busbar for VF6 is 4.5 m long and has approximately 90 nH of inductance and 9 mΩ of resistance.[18] This is only 5% of the value of a twisted wire harness of equal length. Unfortunately, a busbar style connection would be extremely difficult to implement in other sections of the overall harness, like the BOB, thrust stand or thruster. Nonetheless, the final inductance of the discharge circuit is approximately 2.1 μH which is 56% of the inductance a twisted-pair harness of equivalent length.

B. Discharge Voltage Ripple Test

With the improved understanding of the effect of harness impedance and the low-inductance busbar, external inductors were installed in the BOB to "tune" the discharge circuit and artificially increase discharge voltage oscillations at the thruster to assess its effect on performance. Simple air core inductors were built by wrapping loops of wire on an insulator tube and installed in the BOB after C_{DIS}. Tuning inductors, as large as 30 μH, were incrementally added to a thruster operating at 12.5 kW / 600 V resulting P-P voltage oscillations as high as 174 V. However, no noticeable variation in thruster performance was measured.[19]

The current test setups at VF5 and VF6 are tuned so that the maximum discharge voltage oscillations are within maximum allowed magnitude according to AEPS requirements. Further work will be required to assess the impact on voltage ripple on other aspects of the thruster including plume, life, radiated and conducted emissions. During future AEPS integrated system tests the same "tuning" technique can be implemented to simulate the effect of longer harnesses on the system if required.

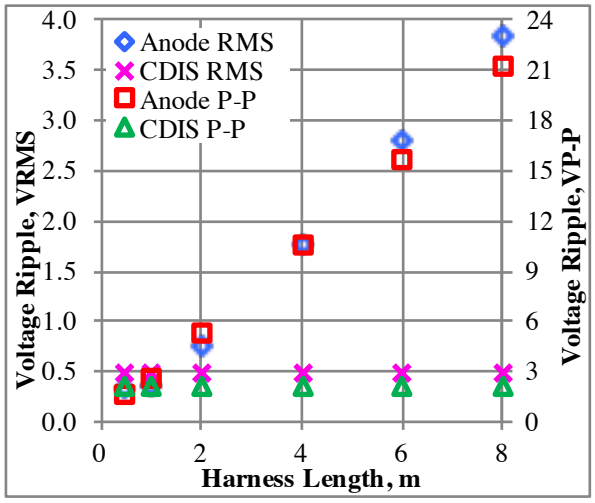

Figure 12. Plot of RMS and P-P voltage ripple as a function of harness length

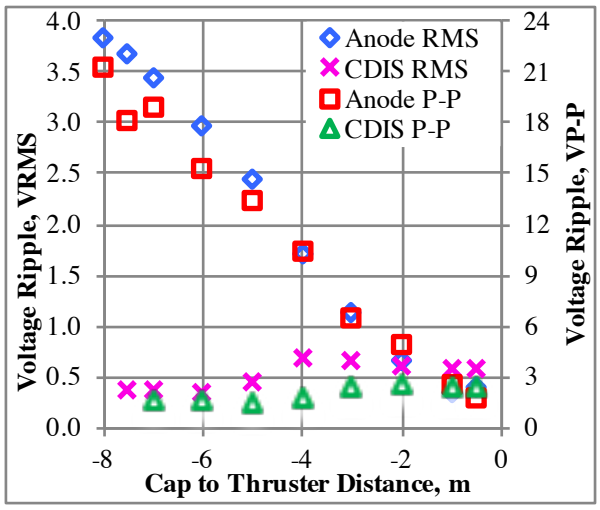

Figure 13. Plot of RMS and P-P voltage ripple as a function of capacitor distance to thruster

V. Conclusion

Experimental measurements and electrical models were used to demonstrate that the primary cause of voltage oscillations of a Hall thruster discharge is the voltage drop generated by the high frequency current oscillations from the thruster flowing through the impedance of the electrical harness. A low inductance between the discharge filter capacitor and the thruster is needed to mitigate voltage ripple at the anode. The discharge filter capacitor should have enough capacitance to supply discharge current oscillations while generating an acceptable amount of voltage ripple. However, increasing the capacitance past that value does not contribute to reduce voltage ripple at the thruster anode.

A simple lumped electrical model with resistive, inductive and capacitive components is a good representation for the harness that connects the thruster to the discharge supply and filter. It effectively predicts the voltage oscillations at the thruster if an accurate representation including high frequency components of the discharge current oscillations are used. This model was used to assess the effectiveness of several inductance reduction techniques including reducing the length of the harness and moving discharge filter capacitor closer to a thruster.

A parallel-plate busbar was effectively used to reduce the harness inductance of experimental test setups at GRC and operate the thruster with low voltage ripple. Using external tuning inductors, the harness inductance was increased to significantly increase voltage ripple at the thruster. However, no significant impact on thruster performance was measured.

References

[1] Smith, B., Nazario, M. and Cunningham, C., "Solar Electric Propulsion Vehicle Demonstration to Support Future Space Exploration Missions," *Space Propulsion 2012*, Bordeaux, France, May 7-10, 2012.

[2] NASA's Journey to Mars, NP-2015-08-2018-HQ, http://www.nasa.gov/sites/default/files/atoms/files/journey-to-mars-next-steps-20151008_508.pdf, 2015.

[3] Manzella, D. and Hack, K., "High-Power Solar Electric Propulsion for Future NASA Missions," AIAA-2014-3718, *50th AIAA/ASME/SAE/ASEE Joint Propulsion Conference*, Cleveland, OH, July 28-30, 2015.

[4] Herman, D., Santiago, W., Kamhawi, H., Polk, J., Snyder, J., Hofer, R. and Sekerak, M., "The Ion Propulsion System for the Asteroid Redirect Robotic Mission," *52nd AIAA/ASME/SAE/ASEE Joint Propulsion Conference*, AIAA 2016-4824, Salt Lake City, Utay, USA, July 25-27, 2016.

[5] Kamhawi, H., Huang, W., Haag, T., Shastry, R., Thomas, R., Yim, J., Herman, D., Williams, G., Myers, J., Hofer, R., Mikellides, I., Sekerak, M. and Polk, J., "Performance Characterization of the Solar Electric Propulsion Technology Demonstration Mission 12.5 kW Hall Thruster," IEPC-2015-007, *30th International Electric Propulsion Conference*, Kobe, Hyogo, Japan, July 4-10, 2015.

[6] Hofer, R., Kamhawi, H., Herman, D., Polk, J., Snyder, J., Mikellides, I., Huang, W. Myers, J., Yim, J., Williams, G., Ortega, A., Jorns, B., Sekerak, M., Griffiths, C., Shastry, R., Haag, T., Verhey, T., Gilliam, B., Katz, I., Goebel, D., Anderson, J., Gilland, J. and Clayman, L., "Development Approach and Status of the 12.5 kW HERMeS Hall Thruster for the Solar Electric Propulsion Technology Demonstration Mission," IEPC-2015-186, *30th International Electric Propulsion Conference*, Kobe, Hyogo, Japan, July 4-10, 2015.

[7] Hofer, R., Kamhawi, H., Mikellides, I., Herman, D., Polk, J., Huang, W., Yim, J., Myers, J. and Shastry, R., "Design Methodology and Scaling of the 12.5 kW HERMeS Hall Thruster for the Solar Electric Propulsion Technology Demonstration Mission," JANNAF-2015-3946, *62st JANNAF Propulsion Meeting*, Nashville, Tennessee, USA, June 1-5, 2015.

[8] Hofer, R. and Kamhawi, H., "Development Status of a 12.5 kW Hall Thruster for the Asteroid Redirect Robotic Mission," *35st International Electric Propulsion Conference,* IEPC-2017-213, Georgia Institute of Technology, USA, October 8-12, 2017.

[9] Piñero, L., Bozak, K., Santiago, W. and Scheidegger, R., "Development of High-Power Hall Thruster Power Processing Units at NASA GRC," *51st AIAA/ASME/SAE/ASEE Joint Propulsion Conference*, AIAA 2015-3921, Orlando, Florida, USA, July 27-30, 2015.

[10] Santiago, W, Bozak, K., Piñero, L., Scheidegger, R., Gonzalez, M., Birchenough, A., Garrett, M. and Ivanov, N., "High Input Voltage, Power Processing Unit Performance Demonstration," *52nd AIAA/ASME/SAE/ASEE Joint Propulsion Conference*, AIAA 2016-5033, Salt Lake City, Utay, USA, July 25-27, 2016.

[11] Herman, D., Tofil, T., Santiago, W., Kamhawi, H., McGuire, M., Polk, J., Snyder, J., Hofer, R., Jackson, J. and Allen, M. "Overview of the Development and Mission Application of the Advanced Electric Propulsion System (AEPS)," *35st International Electric Propulsion Conference,* IEPC-2017-284, Georgia Institute of Technology, USA, October 8-12, 2017.

[12] Choueiri, E., "Plasma Oscillations in Hall Thrusters," *Physics of Plasmas*, Vol. 8, No. 4, pp. 1411-1426, April 2001.

[13] Kim, V., Kozlov, V., Popov, G., and Skrylnikov, A., "Investigation of the Stationary Plasma Thruster Scale Impact on the Electric Filter Parameter Choice," 31st *International Electric Propulsion Conference,* IEPC-99-119, Ann Arbor, Michigan, USA, September 2009.

[14] Randolph, T., Fischer, G., Kahn, J., Gaufman, H., Zhurin, V., Kozubsky, K., and Kim, V., "The Mitigation of Discharge Oscillations in the Stationary Plasma Thruster," *30st AIAA/ASME/SAE/ASEE Joint Propulsion Conference*, AIAA 94-2857, Indianapolis, Indiana, USA, June 27-29, 1994.

[15] Kamhawi, H., Huang, W., Haag, T., Yim, J., Herman, D., Peterson, P., Williams, G., Gilland, J., Hofer, R. and Mikellides, I., "Performance, Facility Pressure Effects, and Stability Characterization Tests of NASA's Hall Effect Rocket with Magnetic Shielding Thruster," *52st AIAA/ASME/SAE/ASEE Joint Propulsion Conference*, AIAA 2016-4826, Salt Lake City, Utah, USA, July 25-27, 2016.

[16] Kamhawi, H., Haag, T., Huang, W. and Hofer, R., "The Voltage-Current Characteristics of the 12.5 kW Hall Effect Rocket with Magnetic Shielding at Different Background Pressure Conditions," *62st JANNAF Propulsion Meeting*, Nashville, Tennessee, USA, June 1-5, 2015.

[17] Snyder, J., Brophy, J., Hofer, R., Goebel, D., and Katz, I., "Experimental Investigation of a Direct-Drive Hall Thruster and Solar Array System," *Journal of Spacecraft and Rockets*, Vol. 51, No. 1, pp. 360-373, January-February 2014.

[18] Peterson, P., Kamhawi, H., Huang, W., Yim, J., Haag, T., Mackey, J., Piñero, L., McVetta, M., Sorrelle, L., Tomsik, T., Gilligan, R. and Herman, D., "NASA Glenn Research Center Vacuum Facility 6 Roconfiguration for HERMeS and AEPS Programs," *35st International Electric Propulsion Conference,* IEPC-2017-028, Georgia Institute of Technology, USA, October 8-12, 2017.

[19] Kamhawi, H., Gilland, J., Williams, G., Mackey, J., Huang, W., Haag, T. and Herman, D., "Performance and Stability Characterization of the HERMeS Thruster with M26 Boron Nitride Discharge Channel," *35st International Electric Propulsion Conference,* IEPC-2017-392, Georgia Institute of Technology, USA, October 8-12, 2017.